

Nuclear shadowing in photoproduction of ρ mesons in ultraperipheral nucleus collisions at RHIC and the LHC

L. Frankfurt,¹ V. Guzey,² M. Strikman,³ and M. Zhalov²

¹*Nuclear Physics Department, School of Physics and Astronomy, Tel Aviv University, 69978 Tel Aviv, Israel*

²*National Research Center “Kurchatov Institute”,*

Petersburg Nuclear Physics Institute (PNPI), Gatchina, 188300, Russia

³*Department of Physics, the Pennsylvania State University, State College, PA 16802, USA*

We argue that with an increase of the collision energy, elastic photoproduction of ρ mesons on nuclei becomes affected by the significant cross section of photon inelastic diffraction which results in the sizable inelastic nuclear shadowing correction to $\sigma_{\gamma A \rightarrow \rho A}$ and by an enhanced contribution of weakly-interacting hadronic configurations in the photon which reduces the effective ρ -nucleon cross section. We take these effects into account by combining the vector meson dominance model, upgraded to include the contribution of high-mass fluctuations according to QCD constraints, with the Gribov–Glauber approximation for nuclear shadowing, where the inelastic nuclear shadowing is included by means of cross section fluctuations. The resulting approach allows us to successfully describe the data on elastic ρ photoproduction on nuclei in heavy ion UPCs in the $7 < W_{\gamma p} < 46$ GeV energy range and to predict the value of the cross section of coherent ρ photoproduction in Pb-Pb UPCs at $\sqrt{s_{NN}} = 5.02$ TeV in Run 2 at the LHC, $d\sigma_{PbPb \rightarrow \rho PbPb}(y=0)/dy = 560 \pm 25$ mb.

I. INTRODUCTION

At high photon beam energies E_γ , the photon participates in the strong interaction with hadrons through its fluctuation into hadronic components. The lifetime of the fluctuations is characterized by the coherence length $l_c = 2E_\gamma/M^2$, where M is the mass of a given component. With an increase of E_γ , l_c increases and becomes larger than the target size R_T for progressively heavier hadronic fluctuations of the photon, which means that the photon can be represented as a coherent superposition of hadronic fluctuations interacting with the target with a wide spectrum of cross sections. This picture can be implemented in terms of either hadronic (vector mesons) or partonic (quark–antiquark dipoles) degrees of freedom.

In the 60’s and early 70’s, it was suggested that the observed hadron-like behavior of a photon in photon–hadron interactions can be represented by the vector meson dominance model (VMD), which assumes that the photon fluctuates into ρ , ω and ϕ mesons that subsequently interact with hadrons [1–3]. The VMD model successfully explained the behavior of the pion form factor, certain features of the nucleon form factors at small momentum transfers and the major part ($\approx 80\%$) of the real photon–nucleon total cross section $\sigma_{\gamma p}$. Combining VMD, the constituent quark model and the Regge–Gribov theory of high energy hadron–hadron scattering, the concept of soft Pomeron phenomenology had been developed and actively used [4, 5] to study properties of the vector meson interaction with nucleons in light vector meson photoproduction and electroproduction at very small momentum transfers Q^2 . One of the key features of this approach is the assumption that $\sigma_{\rho N} = \sigma_{\pi N}$, which is based on the additive quark model ($\sigma_{\rho N}$ and $\sigma_{\pi N}$ are the total ρ -nucleon and pion–nucleon cross sections, respectively). In a wide range of pion energies, the total pion–nucleon cross section is well described by a sum of the soft Pomeron and the secondary Reggeon exchanges [4, 5] (we refer to this model as DL94).

An increase of the photon virtuality Q^2 leads to a gradual transition from the soft nonperturbative QCD regime to the perturbative one, which is clearly revealed in HERA measurements of vector meson electroproduction on the proton at high energies [6]. To explain in a consistent way the $\approx 20\%$ discrepancy between the experimental value of $\sigma_{\gamma p}$ and VMD predictions and the behavior of photon-induced processes with an increase of Q^2 , new theoretical approaches have been developed. On the one hand, within the framework of hadronic description, the VMD model was generalized on the basis of the mass dispersion relation to include higher-mass resonances and the continuum with taking into account both diagonal and non-diagonal transitions between different hadronic states [7–9]; the resulting approach is referred to as the generalized vector meson dominance (GVMD) model. On the other hand, in the perturbative QCD framework, the photon wave function in the strong interaction can be modeled as a superposition of quark–antiquark pairs (dipoles), which interact with the target; the resulting approach is called the color dipole model (CDM) and is best applied to processes with a hard scale, when the bulk of the color dipole–target amplitude can be calculated in perturbative QCD, for the review and references, see, e.g. [6].

From the point of view of the quark–hadron duality these two approaches should be in principle equivalent, but this equivalence is destroyed in their practical realization. In particular, to apply the CDM in the nonperturbative domain, for example, for the description of photoproduction of light vector mesons, the approach should be generalized to take into account more complicated than $q\bar{q}$ states involving gluons ($q\bar{q}g$, etc. whose contributions can be neglected at

large Q^2 in the leading logarithmic approximation) and also to model the cross section of the interaction of large-size dipoles with nucleons. On the other hand, the GVMD model includes coupling constants of the photon to higher-mass resonances and amplitudes of their diagonal and non-diagonal transitions, which are in general unknown. As a result, both approaches require to use phenomenology and engage additional experimental information.

Coherent photoproduction of light vector mesons on nuclear targets at low and intermediate energies has been considered as theoretically well understood within the framework of the VMD model and the Glauber theory of multiple scattering [10] (for brevity, we refer to the resulting approach as VMD-GM). Recently the ALICE collaboration presented results on exclusive ρ meson production at the central rapidity in Pb-Pb ultraperipheral collisions (UPCs) at $\sqrt{s_{NN}} = 2.76$ TeV [11]. The value of the cross section of coherent ρ meson photoproduction on lead at the photon–nucleon center-of-mass energy of $W_{\gamma p} \approx 46$ GeV extracted from this measurement is $\sigma_{\gamma Pb \rightarrow \rho Pb} \approx 2$ mb, which is very close to the $\gamma Au \rightarrow \rho Au$ cross sections in the range of energies of $W_{\gamma p} \approx 7 - 12$ GeV obtained by the STAR collaboration in ion–ion UPCs at RHIC [12–14]. While the calculations of the standard elastic nuclear shadowing in the Glauber model capture the bulk of the nuclear suppression by the factor of approximately four, the experimental values are still significantly, by the factor of approximately 1.5–1.7, smaller than the VMD-GM predictions of [15–17].

The aim of this paper is to generalize the VMD-GM approach by modifying both VMD and Glauber models to take into account the QCD-motivated phenomena that become essential in elastic ρ meson photoproduction on nuclei with an increase of the photon energy: (i) an increasing role of the inelastic nuclear shadowing, and (ii) an enhancement of weakly-interacting configurations contributing to the photon– ρ meson cross section.

At high energies, the Glauber model is substituted by the Gribov–Glauber approach [18] which takes into account both elastic and the inelastic diffraction in the intermediate states contributing to the shadowing correction. Note that in spite of very different pictures of the space–time evolution of the scattering process at moderate and high energies, the expressions for the shadowing correction to hadron–nucleus cross sections look similar in the two approaches. In particular, the nuclear shadowing term is calculable in terms of the elementary hadron–nucleon diffractive cross section, which includes the elastic hadron–nucleon scattering leading to the elastic nuclear shadowing correction of the Glauber model and the inelastic hadron–nucleon scattering. With an increase of energy, inelastic diffraction becomes essential and this results in Gribov’s inelastic nuclear shadowing (GINS) correction.

While an increase of the GINS correction with energy is well-known in the discussed energy range, it is not often appreciated that the relative magnitude of the effect is larger for projectiles with smaller hadron–nucleon cross sections (transverse sizes). Indeed, in proton–nucleus scattering, the GINS correction to the total proton–nucleus cross sections is found to be small [19, 20]. As a consequence, the Glauber model is now widely used in the analysis and interpretation of the data on high energy heavy ion collisions at RHIC and the LHC. For pion–nucleus scattering, the analysis of total pion–deuteron [21] and pion–nucleus [22] cross sections demonstrated that the inelastic nuclear shadowing correction is larger than in the proton–nucleus interaction.

The point-like coupling of the photon to quarks in QCD suggests that the relative contribution of weakly-interacting quark–gluon configurations in the ρ meson produced by the photon is larger than that in the pion produced in soft hadron interactions. This should lead to a certain decrease of the effective ρ –nucleon cross section comparing to $\sigma_{\pi N}$. This results in an overall decrease of the $\gamma A \rightarrow \rho A$ cross section and the relative increase of the GINS correction. Besides, the effect of the inelastic shadowing correction in the elastic cross section is larger than that in the total cross section. Hence, these modifications of the VMD-GM approach noticeably reduce the cross section of coherent ρ photoproduction on nuclei.

To implement these effects in our calculations, we (i) use the framework of cross section fluctuations [23–28] taking into account general properties of the QCD dynamics of bound states and hard processes [26] and the information on inelastic diffraction in proton, pion and photon scattering off a nucleon target, and (ii) modify the VMD model to effectively include the effect of the reduction of the ρ –nucleon cross section. The resulting approach allows us to describe well the data on elastic ρ photoproduction on nuclei in heavy ion UPCs in the $7 < W_{\gamma p} < 46$ GeV energy range in a way consistent with the $\gamma p \rightarrow \rho p$ HERA 2006 data [29], and, thus, to explain away the discrepancy between the data on the $\gamma A \rightarrow \rho A$ cross section and its theoretical description in the VMD-GM approach.

II. CROSS SECTION OF ρ PHOTOPRODUCTION OFF NUCLEAR TARGETS FROM STAR AND ALICE UPC MEASUREMENTS

The basic expression for the cross section of vector meson V photoproduction in nucleus–nucleus UPCs (for review of the physics of ultraperipheral collisions and references, see [30]) reads:

$$\frac{d\sigma_{AA \rightarrow AAV}(y)}{dy} = N_{\gamma/A}(y)\sigma_{\gamma A \rightarrow VA}(y) + N_{\gamma/A}(-y)\sigma_{\gamma A \rightarrow VA}(-y), \quad (1)$$

where $y = \ln(2\omega/M_V)$ is the rapidity of the vector meson; ω is the photon energy; M_V is the vector meson mass; $\sigma_{\gamma A \rightarrow V A}$ is the cross section of exclusive coherent photoproduction of V on nucleus A ; $N_{\gamma/A}(y)$ is the photon flux. The presence of two terms in Eq. (1) is the reflection of the fact that each colliding nucleus can serve as a photon source and as a target.

The flux of photons produced by a fast-moving point-like charge is well-known from classical electrodynamics:

$$N_{\gamma/A}(y) = \frac{2Z^2\alpha_{\text{e.m.}}}{\pi} \left[\zeta K_0(\zeta)K_1(\zeta) - \frac{\zeta^2}{2} (K_1^2(\zeta) - K_0^2(\zeta)) \right], \quad (2)$$

where Z is the nucleus charge; $\alpha_{\text{e.m.}}$ is the fine-structure constant; K_0 and K_1 are modified Bessel functions of the second kind; $\zeta = M_V b_{\min} e^{-y} / (2\gamma_L)$, where γ_L is the nucleus Lorentz factor and b_{\min} is the minimal impact parameter of the nucleus–nucleus ultraperipheral collision. The photon flux calculated using Eq. (2) with $b_{\min} = 2R_A$ (R_A is the nuclear radius) reproduces with the precision of a few percent a more accurate calculation, which takes into account the nuclear form factor and the suppression of the strong nucleus–nucleus interaction calculated using the Glauber model.

At $y = 0$, the two terms in Eq. (1) are equal and one can then unambiguously determine the $\gamma A \rightarrow \rho A$ cross section using the experimental values of the $d\sigma_{AA \rightarrow AA\rho}(y = 0)/dy$ cross section measured by the STAR collaboration at RHIC [12–14] and the ALICE collaboration at the LHC [11]:

$$\sigma_{\gamma A \rightarrow \rho A}(W_{\gamma p}) = \frac{1}{2N_{\gamma/A}(y = 0)} \frac{d\sigma_{AA \rightarrow AA\rho}(y = 0)}{dy}, \quad (3)$$

where $W_{\gamma p} \equiv W_{\gamma p}(y = 0) = \sqrt{2M_\rho m_N \gamma_L}$ with $M_\rho = 770$ MeV being the ρ meson mass and m_N the nucleon mass. The $\gamma A \rightarrow \rho A$ cross section determined this way is presented in Table I as a function of the corresponding $W_{\gamma p}$.

Nuclear target	$W_{\gamma p}$, GeV	$\sigma_{\gamma A \rightarrow \rho A}$, mb
$\gamma Au \rightarrow \rho Au$	6.96	2.08 ± 0.33
$\gamma Au \rightarrow \rho Au$	10.04	1.9 ± 0.76
$\gamma Au \rightarrow \rho Au$	12.46	1.58 ± 0.25
$\gamma Pb \rightarrow \rho Pb$	46.28	1.97 ± 0.21

TABLE I: The cross sections of ρ photoproduction on nuclear targets extracted from the STAR [12–14] and the ALICE UPC measurements [11].

III. NUCLEAR SHADOWING IN ρ PHOTOPRODUCTION ON NUCLEAR TARGETS

In the Glauber model, the cross section of coherent ρ photoproduction on nuclei reads [1]:

$$\sigma_{\gamma A \rightarrow \rho A}^{\text{VMD}} = \frac{d\sigma_{\gamma p \rightarrow \rho p}(t = 0)}{dt} \int_{-\infty}^{t_{\min}} dt \left| \int d^2 \vec{b} e^{i\vec{q}_\perp \cdot \vec{b}} \int dz \rho_A(b, z) e^{iq_\parallel z} e^{-(1-i\eta) \frac{\sigma_{\rho N}}{2} \int_z^\infty dz' \rho_A(b, z')} \right|^2, \quad (4)$$

where $\sigma_{\rho N}$ is the total ρ –nucleon cross section; η is the ratio of the real to the imaginary parts of the ρ –nucleon scattering amplitude; \vec{q}_\perp and q_\parallel are the transverse and longitudinal components of the momentum transfer to the nucleus, respectively; ρ_A is the nuclear density normalized by the relation $\int dz d^2 \vec{b} \rho_A(b, z) = A$. The nuclear density is well known from studies of elastic electron and proton scattering on nuclei at intermediate energies (see, for example, [31–33]). In our calculations we used the Hartree–Fock–Skyrme nuclear density which describes the root-mean-square radii of nuclei across the periodic table with the precision better than 2%. The minimal momentum transferred squared is $t_{\min} = -(M_\rho^2 m_N / W_{\gamma p}^2)^2 = -(q_\parallel)^2$, where $W_{\gamma p}$ is the invariant photon–nucleon energy ($W_{\gamma p}^2 = 2m_N E_\gamma + m_N^2$ in the laboratory frame). In the VMD model, the forward elementary $\gamma p \rightarrow \rho p$ cross section in Eq. (4) can be related to the total ρN cross section, $\sigma_{\rho N}$, using the optical theorem:

$$\frac{d\sigma_{\gamma p \rightarrow \rho p}(t = 0)}{dt} = \frac{1}{16\pi} \left(\frac{e}{f_\rho} \right)^2 (1 + \eta^2) \sigma_{\rho N}^2, \quad (5)$$

where f_ρ is the $\gamma - \rho$ coupling constant ($f_\rho^2/4\pi = 2.01 \pm 0.1$) fixed by the $\Gamma(\rho \rightarrow e^+ e^-)$ width of the $\rho \rightarrow e^+ e^-$ decay. Note also that the effect of $t_{\min} \neq 0$ in $d\sigma_{\gamma p \rightarrow \rho p}(t = 0)/dt$ is negligibly small and can be neglected.

At high photon energies, neglecting the effects of $q_{\parallel} \neq 0$ and $\eta \neq 0$ (in the $5 \text{ GeV} < W_{\gamma p} < 50 \text{ GeV}$ range, $|\eta| < 0.1$ and thus can be safely neglected [4]) in Eq. (4), one can write it in the form of the optical limit of the Glauber model:

$$\sigma_{\gamma A \rightarrow \rho A}^{\text{VMD}} = \left(\frac{e}{f_{\rho}} \right)^2 \int d^2 \vec{b} \left| 1 - e^{-\frac{\sigma_{\rho N}}{2} T_A(b)} \right|^2 = \left(\frac{e}{f_{\rho}} \right)^2 \sigma_{\rho A}^{\text{el}}, \quad (6)$$

where $T_A(b) = \int dz \rho_A(b, z)$.

The interpretation of Eq. (6) is straightforward and well-known: the incoming photon transforms into a ρ meson far before the target and then the ρ meson coherently interacts with the nucleons along its trajectory. The Glauber model takes into account the elastic nuclear shadowing effect, which depends on the total ρN cross section. Based on the additive quark model, it is generally assumed that $\sigma_{\rho N}(W) = \sigma_{\pi N}(W) = [\sigma_{\pi^+ N}(W) + \sigma_{\pi^- N}(W)]/2$. The experimental pion-nucleon cross sections in a wide range of energies are well described as a simple sum of the soft Pomeron and the secondary Reggeon exchanges [4]. Correspondingly, this resulted in a simple form (DL94) for the energy dependence of $\sigma_{\rho N}$ [5]:

$$\sigma_{\rho N}(W) = 13.6 W^{2(\alpha_P(0)-1)} + 31.8 W^{2(\alpha_R(0)-1)}, \quad (7)$$

where $\alpha_R(t) = 0.55 + 0.93t$ is the Reggeon exchange trajectory; $\alpha_P(t) = 1.0808 + 0.25t$ is the soft Pomeron trajectory (Donnachie-Landshoff pomeron) characterizing the high energy behavior of soft hadron-nucleon processes. Since the DL94 model did not fit well the forward ρ photoproduction cross section on the proton measured to that time in low energy experiments [34–36] and in the ZEUS experiment [37–39] at high energies, Donnachie and Landshoff suggested [40] to simply renormalize the forward cross section [Eq. (5)] by the factor of 0.84 motivated by possible corrections to the $\gamma - \rho$ coupling constant (this renormalization was consistent with large experimental uncertainties of the data).

In Fig. 1 we compare the total cross sections of coherent ρ photoproduction extracted from the STAR and ALICE measurements (see Table I) to those calculated in the impulse approximation (IA), when all nuclear effects except for coherence are neglected (blue dot-dashed line), and in the Glauber model (red dashed line) using the DL94 ρN total cross section (Eq. (7)). From the figure one finds that the VMD-GM with the DL94 model for $\sigma_{\rho N}$ predicts the suppression of $\sigma_{\gamma A \rightarrow \rho A}$ by approximately a factor of four compared to the IA calculation, but it still overestimates the experimental cross sections by the factor of 1.5 – 2. Besides, the energy dependence is different: while the calculated cross sections slowly grow with energy, the experimental values slightly decrease or stay almost constant. Note that the calculated values of the $\gamma Au \rightarrow \rho Au$ cross section are smaller than those for the lead target by approximately 5% for all energies. Hence, we neglect this difference throughout our paper and perform our calculations for lead keeping in mind the 5% reduction of the nuclear cross section when we compare our calculations with the STAR data.

To check the accuracy of the Glauber model calculations in Eq. (6) in combination with the DL94 pion-nucleon cross section, we calculated the hadron-nucleus total and inelastic cross sections for the neutron and pion projectiles in the Glauber approach:

$$\begin{aligned} \sigma_{hA}^{\text{tot}} &= 2 \int d^2 \vec{b} \left[1 - e^{-\frac{\sigma_{hN}}{2} T_A(b)} \right], \\ \sigma_{hA}^{\text{in}} &= \int d^2 \vec{b} \left[1 - e^{-\sigma_{hN} T_A(b)} \right]. \end{aligned} \quad (8)$$

The neutron-nucleon cross section σ_{nN} is estimated using the additive quark model counting rule relation [41] $\sigma_{nN} = 3/2 \sigma_{\pi N}$, where the pion-nucleon cross section is given by Eq. (7). The results of our calculations are compared to the data [22, 42–44] in Fig. 2. One can see from the figure that the calculations agree very well with the measurements. This means that the reasons of the disagreement of similar calculations of the $\gamma A \rightarrow \rho A$ cross section with the STAR and ALICE data are in specifics of the light vector meson photoproduction process.

This conclusion is confirmed by our observation that the latest 2006 H1 data on the $\gamma p \rightarrow p \rho$ cross section [29] (we extrapolated the H1 cross sections given at $-t = 0.01 \text{ GeV}^2$ to $-t = 0$ assuming the e^{Bt} dependence with the value of the slope B reported by H1) disagrees with the normalization of the forward cross section calculated using the DL94 model by the factor of 0.84. This is seen in Fig. 3, where the forward $\gamma p \rightarrow p \rho$ cross section evaluated using Eqs. (5) and (7) (the green dot-dashed curve labelled “VMD-DL94”) is compared to the whole bulk of the data. Also, for comparison, we show the parametrization of the forward $\gamma p \rightarrow p \rho$ cross section from the Starlight Monte-Carlo generator [45], which is widely used for predictions and modeling of vector meson photoproduction on nuclear targets. In order to agree with the 2006 H1 data, the results of the VMD-DL94 and the Starlight parametrization should be decreased by the factor of approximately 0.7, which is much larger than what could be allowed by a variation of f_{ρ} . From the analysis presented above we can conclude the following: the assumption of the ρ meson dominance in the

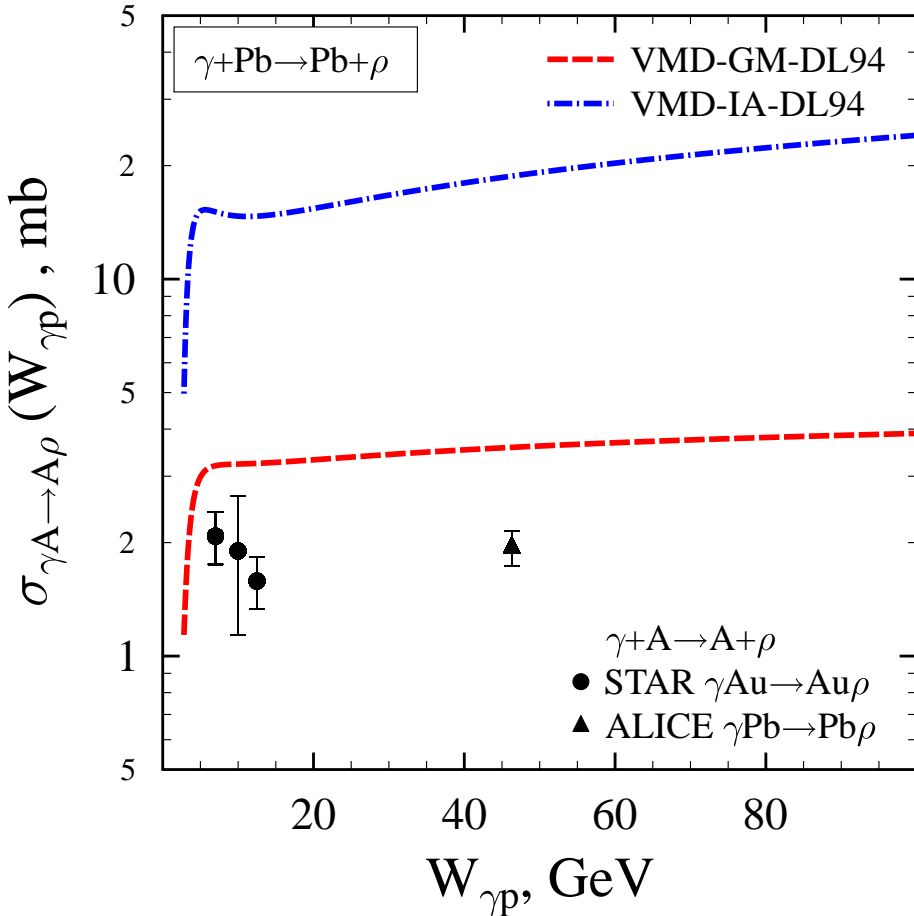


FIG. 1: The $\gamma A \rightarrow \rho A$ cross section as a function of $W_{\gamma p}$. The VMD-GM (the red dashed curve) and VMD-IA (blue dot-dashed line) predictions for a ^{208}Pb target based on the DL94 parametrization of the ρN cross section are compared to the experimental values extracted from the STAR and ALICE UPC measurements.

photon wave function has to be modified in order to agree to the whole set of data including the results of 2006 H1 measurements.

To this end, one can write the ρ meson photoproduction amplitude as the dispersion integral over the masses of the intermediate states generated in the $\gamma \rightarrow M$ transitions, which will involve the on-mass-shell f_ρ and the physical ρN cross section. It is possible to demonstrate that inclusion of the contribution of the higher states can only weakly change f_ρ , but it can significantly reduce the cross section of the ρ meson production. Hence, the effective ρ -nucleon cross section $\hat{\sigma}_{\rho N}$ should be smaller than $\sigma_{\rho N} = \sigma_{\pi N}$. We assume that $\hat{\sigma}_{\rho N}$ can be extracted from the requirement that Eq. (5) describes reasonably well the experimentally measured forward $\gamma p \rightarrow \rho p$ cross section:

$$\hat{\sigma}_{\rho N}(W_{\gamma p}) = \frac{f_\rho}{e} \sqrt{16\pi \frac{d\sigma_{\gamma p \rightarrow \rho p}^{\text{exp}}(t=0)}{dt}}. \quad (9)$$

This way we effectively take into account the enhanced contribution of the components in the ρ meson wave function that interact with the strength weaker than the average one. This effect is present in the CDM and can also be modeled by non-diagonal transitions among different hadronic components of the photon and the ρ meson in the

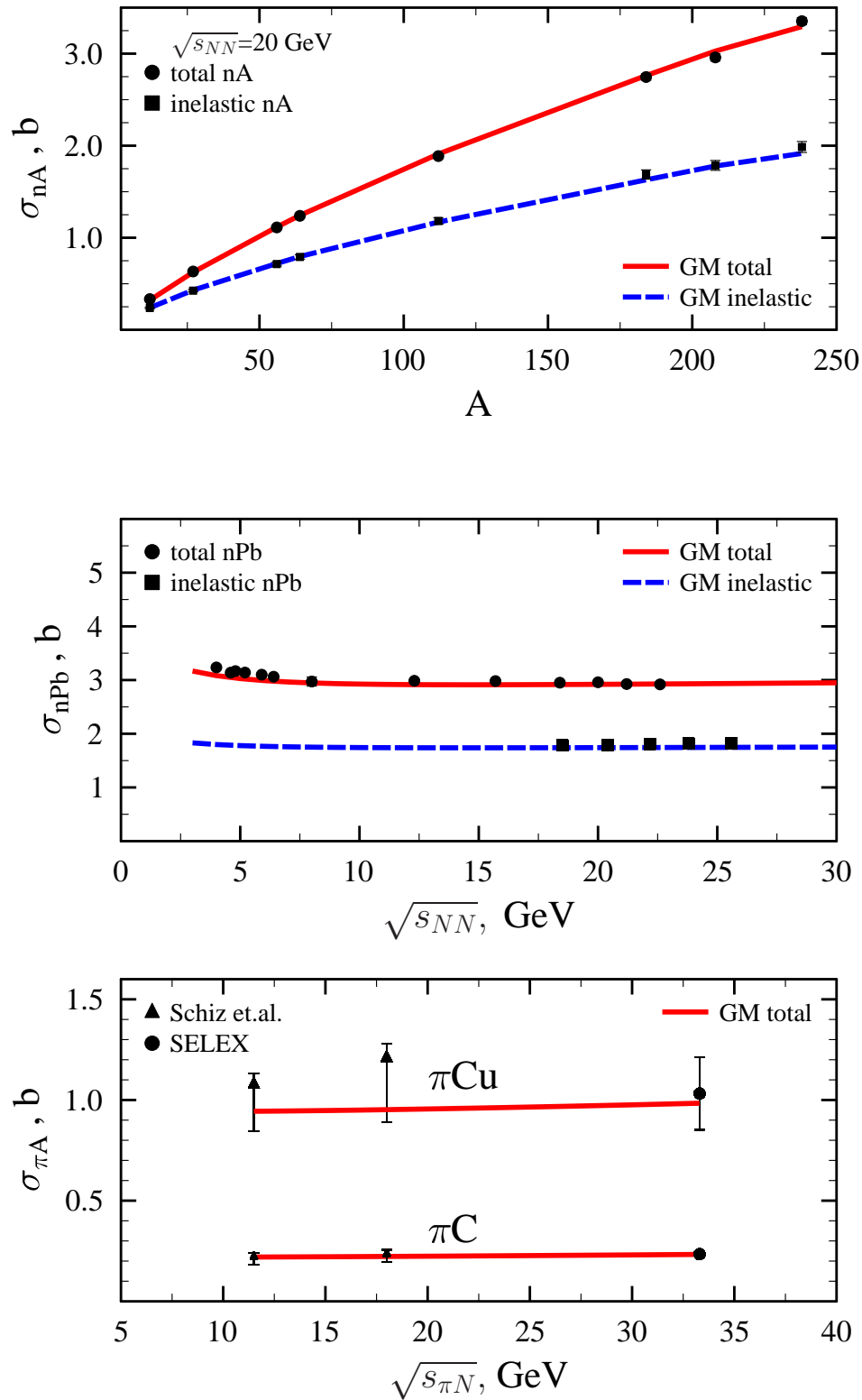


FIG. 2: Upper and middle: Comparison of the total and inelastic neutron–nucleus cross sections calculated in the Glauber model with the available data. Bottom: The total pion–nucleus cross section as a function of $\sqrt{s_{\pi N}}$: the Glauber model calculations with the DL94 model for $\sigma_{\pi N}$ are compared to the available data.

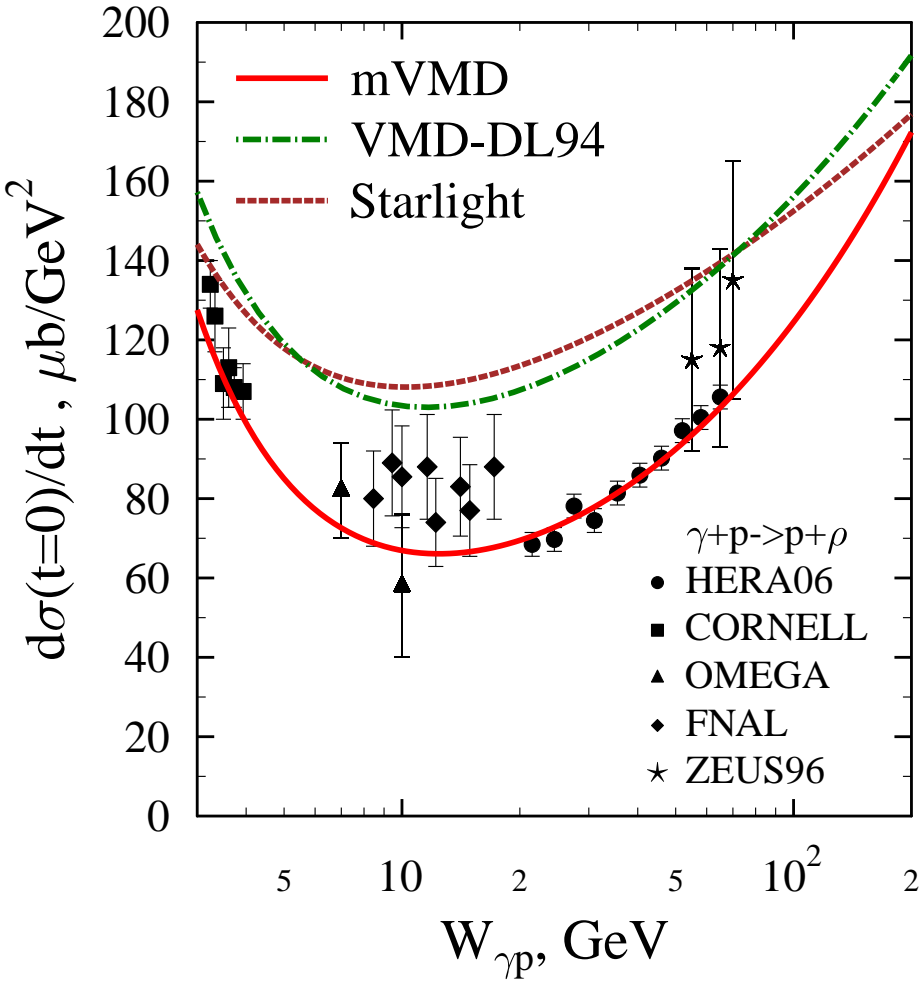


FIG. 3: Comparison of the experimentally measured forward cross section of coherent ρ photoproduction on the proton [29, 34–39] with the VDM-DL94 model and the Starlight parametrization. The red solid line shows the modified VMD (mVMD) parametrization (see text for details).

GVMD approach. We refer to this model as the modified vector meson dominance (mVMD) model; it is shown by the solid red curve in Fig. 3.

The Gribov–Glauber model takes into account both elastic and inelastic diffraction; the latter leads to the additional—as compared to the Glauber model—inelastic nuclear shadowing contribution (the Gribov shadowing correction) [18]. The standard method to do this is given by the formalism of cross section fluctuations, which conveniently and successfully describes diffractive dissociation of protons, neutrons and pions on hydrogen and nuclei and inelastic nuclear shadowing in hadron–nucleus total cross sections [46].

Applying this formalism to the ρ meson–nucleus scattering, we obtain:

$$\sigma_{\gamma A \rightarrow \rho A}^{\text{mVMD-GGM}} = \left(\frac{e}{f_\rho} \right)^2 \int d^2 \vec{b} \left| \int d\sigma P(\sigma) \left(1 - e^{-\frac{\sigma}{2} T_A(b)} \right) \right|^2, \quad (10)$$

which generalizes Eq. (6).

The interpretation of Eq. (10) is the following: the photon fluctuates into the ρ meson, which interacts with the target as a coherent superposition of eigenstates of the scattering operator, whose eigenvalues are the scattering cross

sections σ ; the weight of a given fluctuation is given by the distribution $P(\sigma)$. Each state interacts with nucleons of the target nucleus according to the Gribov–Glauber model. The result is summed over all possible fluctuations, which corresponds to averaging with the distribution $P(\sigma)$ at the amplitude level.

Based on the similarity between the pion and ρ meson wave functions suggested by the additive quark model and our discussion above it is natural to assume that $P(\sigma)$ for the ρN interaction should be similar to the pion $P_\pi(\sigma)$, which we additionally multiply by the factor of $1/(1 + (\sigma/\sigma_0)^2)$ to take into account the enhanced contribution of small σ in the ρN interaction:

$$P(\sigma) = C \frac{1}{1 + (\sigma/\sigma_0)^2} e^{-(\sigma/\sigma_0 - 1)^2/\Omega^2}. \quad (11)$$

The parameterization of Eq. (11) satisfies the basic QCD constraint $P(\sigma = 0) \neq 0$ and also $P(\sigma \rightarrow \infty) \rightarrow 0$. The free parameters C , σ_0 and Ω are found from the constraints:

$$\begin{aligned} \int d\sigma P(\sigma) &= 1, \\ \int d\sigma P(\sigma)\sigma &= \langle\sigma\rangle, \\ \int d\sigma P(\sigma)\sigma^2 &= \langle\sigma\rangle^2(1 + \omega_\sigma), \end{aligned} \quad (12)$$

where $\langle\sigma\rangle = \hat{\sigma}_{\rho N}$ in the mVMD model.

The quantity ω_σ parametrizes the dispersion of $P(\sigma)$ around its mean value $\langle\sigma\rangle$, i.e., it characterizes the strength of cross section fluctuations. It can be determined using experimental information on the photon diffraction dissociation, in particular, the factorization of the photon and the pion diffraction dissociation cross sections scaled by the respective total cross sections. In detail, the measurement [47] of inclusive diffraction dissociation of photons on hydrogen, $\gamma p \rightarrow X p$, in the range of $75 < E_\gamma < 148$ GeV and $M_X^2/s < 0.1$ (M_X denotes the produced diffractive mass) and the control measurement of inclusive diffraction dissociation of pions in the $\pi p \rightarrow X p$ reaction at $E_\pi = 100$ GeV showed that the respective M_X^2 distributions scaled by the total cross sections are very similar in the photon and pion cases. For the cross sections integrated over M_X^2 , this observation means that:

$$\frac{d\sigma_{\gamma p \rightarrow X p}(t = 0)/dt}{\sigma_{\gamma p}} \approx \frac{d\sigma_{\pi p \rightarrow X p}(t = 0)/dt}{\sigma_{\pi p}} = \frac{\omega_\sigma^\pi}{16\pi} \sigma_{\pi N}, \quad (13)$$

where in the last equation we expressed the cross section of pion diffraction dissociation in terms of ω_σ^π characterizing the $P_\pi(\sigma)$ distribution and the total pion–nucleon cross section $\sigma_{\pi N}$.

On the other hand, using the formalism of cross section fluctuations for the ρ –nucleon scattering and the mVMD model for the $\gamma - \rho$ transition, we obtain for the cross section of photon diffraction dissociation [compare to Eq. (5)]:

$$\frac{d\sigma_{\gamma p \rightarrow X p}(t = 0)}{dt} = \frac{1}{16\pi} \left(\frac{e}{f_\rho} \right)^2 \left[\int d\sigma P(\sigma)\sigma^2 - (\hat{\sigma}_{\rho N})^2 \right] = \frac{\omega_\sigma}{16\pi} \left(\frac{e}{f_\rho} \right)^2 (\hat{\sigma}_{\rho N})^2, \quad (14)$$

where the diffraction dissociation final state X by construction does not contain ρ . Substituting Eq. (14) in Eq. (13) we obtain the desired constraint on ω_σ :

$$\omega_\sigma = \frac{f_\rho^2}{e^2} \frac{\sigma_{\pi N} \sigma_{\gamma p}}{\hat{\sigma}_{\rho N}^2} \omega_\sigma^\pi, \quad (15)$$

where the total photon–proton cross section $\sigma_{\gamma p}$ is taken from the fit to data [4].

For the pion projectile, we use the constituent quark counting rule for the ratio of the nucleon–nucleon and the pion–nucleon total cross sections and obtain:

$$\omega_\sigma^\pi(s) = \frac{3}{2} \omega_\sigma^N(s). \quad (16)$$

Here we effectively use validity of the limiting fragmentation which is well established experimentally.

The pattern of cross section fluctuations for the nucleon projectile has the following dependence of the invariant collision energy \sqrt{s} : the cross section fluctuations reach a broad maximum for $24 < \sqrt{s} < 200$ GeV, are most likely small for $\sqrt{s} < 24$ GeV and gradually decrease for $\sqrt{s} > 200$ GeV toward the Tevatron and LHC energies. Therefore, we use the following parametrization for the parameter ω_σ^N describing the dispersion of the fluctuations:

$$\omega_\sigma^N(s) = \begin{cases} \beta \sqrt{s}/24, & \sqrt{s} < 24 \text{ GeV} \\ \beta, & 24 < \sqrt{s} < 200 \text{ GeV} \\ \beta - 0.15 \ln(\sqrt{s}/200) + 0.03(\ln(\sqrt{s}/200))^2, & \sqrt{s} > 200 \text{ GeV}. \end{cases} \quad (17)$$

where the parameter $\beta \approx 0.25 - 0.35$ was determined from the analysis of pp and $\bar{p}p$ data [26].

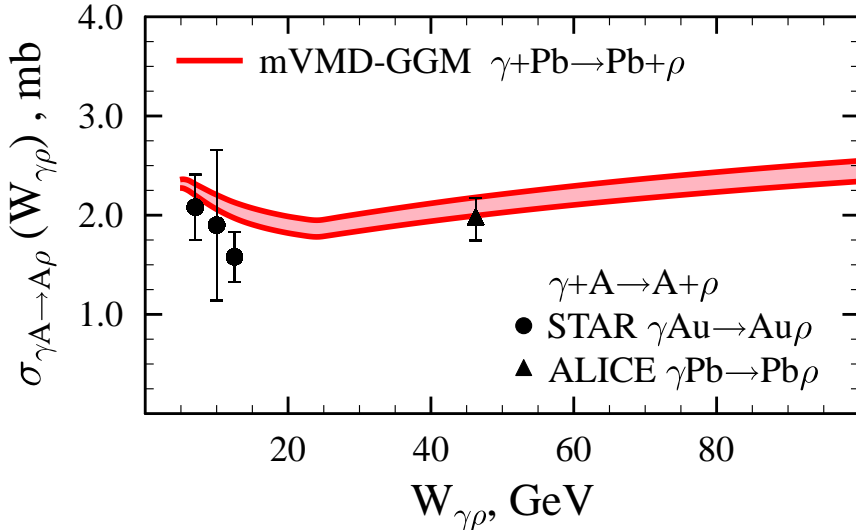


FIG. 4: The $\sigma_{\gamma A \rightarrow \rho A}$ cross section as a function of $W_{\gamma p}$. The theoretical predictions using the mVMD model for the $\gamma p \rightarrow \rho p$ cross section and the Gribov-Glauber model with cross section fluctuations for the $\gamma A \rightarrow \rho A$ amplitude are compared to the STAR (circle) and ALICE (triangle) data. The shaded area reflects the theoretical uncertainty associated with the parameter β characterizing the strength of cross section fluctuations (see text for details).

It is known [19] from studies of corrections to the Glauber model for total proton–nucleus cross sections that suppression due to the inelastic shadowing is almost compensated by the effect of short-range correlations (SRC) in the wave function of the target nucleus. We included the effect of SRC by the following replacement [48]:

$$T_A(b) \rightarrow T_A(b) + \xi_c \frac{\sigma_{\rho N}}{2} \int dz \rho_A^2(b, z), \quad (18)$$

where $\xi_c = 0.74$ fm is the correlation length.

Our predictions for the $\gamma A \rightarrow \rho A$ cross section as a function of $W_{\gamma p}$ are presented in Fig. 4. The red solid curve presents the results of the calculation using the mVMD model for the $\gamma p \rightarrow \rho p$ cross section and the Gribov–Glauber model with the effect of cross section fluctuations, see Eq. (10). The shaded area shows the uncertainty of our calculations due to the variation of the fluctuation strength ω_σ by changing β in the range $0.25 \leq \beta \leq 0.35$. The theoretical curve is compared to the STAR (circle) and ALICE (triangle) data. One can clearly see from the figure that the inclusion of the inelastic nuclear shadowing enables us to explain the discrepancy between the UPC data on coherent ρ photoproduction on nuclei at large $W_{\gamma p}$ and the theoretical description of this process in the framework of the VMD-GM with the DL94 parametrization of the ρN cross section.

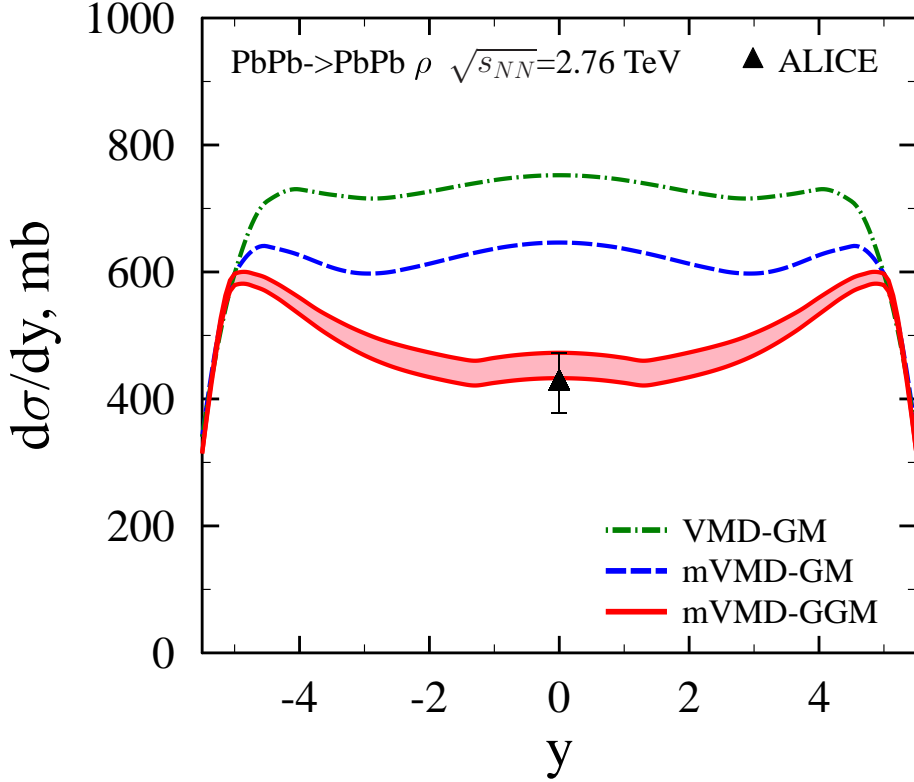


FIG. 5: The rapidity distribution of coherent ρ photoproduction in Pb-Pb UPCs at $\sqrt{s} = 2.76$ TeV. Theoretical predictions of the mVMD-GGM (red solid curves with the shaded area showing the uncertainty due to the variation of the fluctuation strength), the mVMD-GM (blue dashed curve) and the VMD-GM (green dot-dashed curve) are compared to the ALICE data (see text for details).

IV. DISCUSSION

The effect of the inelastic shadowing correction, which we demonstrate in these calculations, can be checked in the UPC measurements at the LHC. The inelastic nuclear shadowing dramatically changes the rapidity distribution of coherent ρ photoproduction in ion UPCs. Figure 5 presents the results of our calculation of $d\sigma_{PbPb \rightarrow \rho PbPb}/dy$, see Eq. (1), as a function of the ρ meson rapidity y in Pb-Pb UPCs at the LHC at 2.76 TeV. The red solid curves correspond to the combination of the mVMD model and the Gribov-Glauber model for nuclear shadowing with cross section fluctuations (the shaded area shows the uncertainty of the calculations related to the variation of the fluctuation strength due to the change of β in the range $0.25 \leq \beta \leq 0.35$); the blue dashed curve is the result of the calculation in mVMD-GM, i.e. without cross section fluctuations; the green dot-dashed curve is the result of the VMD-DL94 model combined with the Glauber model. The shape of the rapidity distribution predicted by the mVMD-GGM calculations is due to specifics of symmetric UPCs and the interplay between the energy dependence of the inelastic shadowing correction and the photon flux.

Such a behavior is different from the almost flat distribution obtained in VDM-GM, Starlight and is in stark contrast with the calculations [49, 50] in the color dipole model approach predicting a bell-like shape with the maximum at $y = 0$ and small cross sections at $y \approx -4.5$ corresponding to $W_{\gamma p} \approx 5 - 10$ GeV, i.e., in the energy range of the STAR measurements. From Fig. 4 it is seen that the experimental photoproduction cross section is almost constant in the

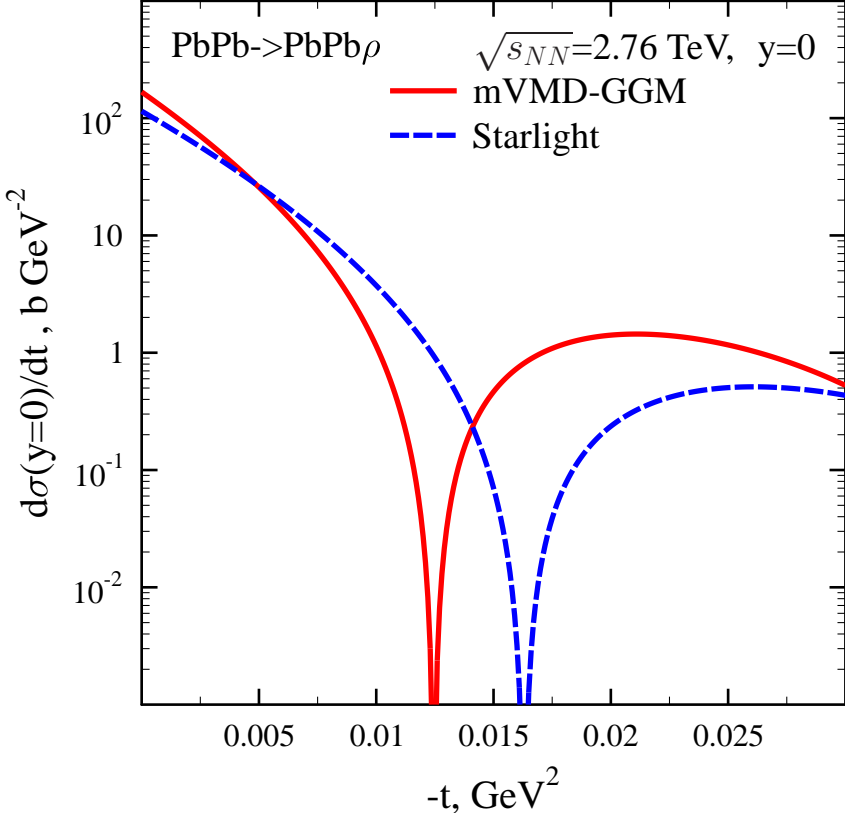


FIG. 6: The momentum transfer distribution of coherent ρ photoproduction in Pb-Pb UPCs at $\sqrt{s} = 2.76$ TeV. The mVMD-GGM prediction (red solid curve) is compared to the Starlight result (blue dashed curve).

energy range spanning the STAR and ALICE energies, $\sigma_{\gamma Pb \rightarrow \rho Pb} \approx 2$ mb. In UPCs at $y = 0$ contributions from both colliding nuclei serving as a target are equal, while at $|y| = 4.5$ only the contribution of the low energy photon dominates. The photon fluxes are calculated in all studies similarly and with good accuracy, $N_{\gamma/Pb}(y = 0) = 108$ and $N_{\gamma/Pb}(y = -4.5) = 250$. Then one easily obtains that $\sigma_{PbPb \rightarrow PbPb\rho}(|y| = 4.5) \approx 500$ mb $> \sigma_{PbPb \rightarrow PbPb\rho}(y = 0) \approx 430$ mb. These estimates confirm that the two-bumped shape of the rapidity distribution seems to be more reasonable.

The good agreement with the ALICE result allows us to predict the value of the cross section of coherent ρ photoproduction in Pb-Pb UPCs at $\sqrt{s_{NN}} = 5.02$ TeV in Run 2 at the LHC:

$$\frac{d\sigma(y = 0)}{dy} = 560 \pm 25 \text{ mb.} \quad (19)$$

Examining the calculations of elastic photoproduction of ρ mesons on nuclei in the dipole model framework [49, 50], one notes that some of them describe the STAR and ALICE data while others do not - the results strongly depend on the models used for ρ -meson wave function and the dipole cross section. The dipole model framework was successfully used in the analyses of hard processes studied at HERA, such as, e.g., deep inelastic scattering (DIS) and vector meson electroproduction, when one can use the QCD factorization theorems to calculate the dipole cross section. At the same time, application of the dipole models to soft processes is much more difficult to justify. Indeed, in this case the interaction involves hadrons in configurations containing large gluonic component and not only the $q\bar{q}$ configuration.

Also, diffraction—even in DIS—requires extension of the dipole approximation to include the $q\bar{q}g$ component. Note that several dipole models use a light quark mass (for example, ~ 10 MeV in [50]) leading to a very large transverse size of the photon wave function and, consequently, to the t -dependence of the Compton elastic scattering which is stronger than that observed in the data [51].

We also would like briefly comment on the description of the STAR and ALICE data in the Starlight Monte-Carlo generator. From our point of view, the observed agreement with the data on coherent ρ meson photoproduction on nuclei is just an effect of lucky coincidence and the weak energy dependence of the photoproduction cross section in the energy range covered by the STAR and ALICE measurements. The Starlight calculations are based on the parametrization of the forward $\gamma p \rightarrow \rho p$ cross section, VMD and the optical theorem. The $\gamma A \rightarrow A\rho$ cross section is calculated in Starlight using the following expression:

$$\sigma_{\gamma A \rightarrow A\rho} = \frac{d\sigma_{\gamma A \rightarrow A\rho}(t=0)}{dt} \int_{-\infty}^{t_{\min}} |F_A(t)|^2 dt = \frac{1}{16\pi} \frac{e^2}{f_\rho^2} [\sigma_{\rho A}^{\text{tot}}]^2 \int_{-\infty}^{t_{\min}} |F_A(t)|^2 dt, \quad (20)$$

where $F_A(t)$ is the nuclear form factor normalized by the condition $F_A(0) = 1$. Note that the factorized form in Eq. (20) is an approximation. While the forward photoproduction cross section on a nuclear target in Eq. (20) follows from the VMD model, the optical theorem and the Glauber model (see Eq. (4)), Eq. (20) does not take into account that the strong absorption of the ρ meson in the central region of a heavy nucleus results in narrowing of the momentum transfer distribution compared to that dictated by the undistorted nuclear form factor. In particular, for heavy nuclei the first diffraction minimum is shifted by 10–15% compared to the position of the dip in the nuclear form factor. This shift is clearly revealed in the momentum transfer distributions at the rapidity $y = 0$ calculated in mVMD-GGM and in Starlight approaches, which are shown in Fig. 6. Qualitatively such an effect is revealed in the data presented by STAR and ALICE.

A more serious shortcoming of the Starlight calculations is the use of the inelastic ρ -nucleus cross section instead of the total cross section in Eq. (20) (compare the expressions in Eq. (8)), which violates the optical theorem. At high energies the cross section of elastic hadron scattering by a heavy nucleus is about 30% of the total cross section (see Fig. 2). As a result, this decreases the estimate of the forward cross section by a factor of about two. One can see from Fig. 3 that the parametrization used in Starlight is close to that given by the DL94 model. Therefore, dividing the value of the VMD-GM cross section (green dot-dashed line) at $y = 0$ by the factor of two we reproduce the Starlight agreement with the ALICE data.

Finally, we would like to emphasize that our calculations use as input the data on the forward ρ photoproduction cross section off the proton and the data on the photon and pion diffraction on hydrogen in a wide range of energies $5 \text{ GeV} \leq W_{\gamma p} \leq 50 \text{ GeV}$. As one can see from Fig. 3, the forward $\gamma p \rightarrow \rho p$ cross section is known in the 5–20 GeV range with rather large experimental errors, while $\sigma_{\rho N}$ extracted from these data is important for calculation of the cross section for the STAR kinematics and for predictions of the rapidity distribution at large $|y|$ at the LHC energies. Some of these measurements would be doable with the recoil detector at COMPASS. Information at higher energies could be obtained from the studies of UPCs in pA at the LHC. It would be also very important to collect data on the photon and pion coherent diffraction off the proton and nuclear targets at high energies since only a handful of such data are available now. In the case of the γA process, one could get this information from UPCs at the LHC.

Other possible directions of studies include coherent ϕ production, where we expect a significant amplification of the inelastic intermediate state effects due to the small value of $\sigma(\phi N)$ (such a measurement is certainly challenging for the main decay channel of ϕ into two kaons, but the 15% $\rho\pi$ channel may work).

The phenomenon of fluctuations of the interaction strength, which we discussed in the context of ρ meson exclusive production on nuclei, should also be manifested in a wide range of high energy γA inelastic processes that could be studied in UPCs at the LHC. Effects of such fluctuations in inelastic pA collisions were considered in [52] with experimental evidence reported in [53].

V. CONCLUSION

With an increase of the collision energy, the composite structure of the photon becomes progressively more pronounced, which leads to the following two features of the calculation of the cross section of ρ meson photoproduction on nuclei compared to the lower energies. First, the significant cross section of photon inelastic diffraction results in the sizable inelastic nuclear shadowing correction to the $\gamma A \rightarrow \rho A$ cross section. Second, the QCD-inspired enhancement of weakly interacting hadronic fluctuations of the photon reduces the effective ρ -nucleon cross section in agreement with the latest 2006 H1 data. We took these features into account by combining the QCD-improved VMD model with the Gribov-Glauber model for nuclear shadowing, where the inelastic nuclear shadowing is included by

means of cross section fluctuations. The resulting approach allows us to successfully describe the data on elastic ρ photoproduction on nuclei in heavy ion UPCs in the $7 < W_{\gamma p} < 46$ GeV energy range and to predict the value of the cross section of coherent ρ photoproduction in Pb-Pb UPCs at $\sqrt{s_{NN}} = 5.02$ TeV in Run 2 at the LHC: $d\sigma_{PbPb \rightarrow \rho PbPb}(y = 0)/dy = 560 \pm 25$ mb.

[1] T. H. Bauer, *et al.*, Rev. Mod. Phys. **50**, 261 (1978) [Erratum-ibid. **51**, 407 (1979)].
[2] J. J. Sakurai, Annals Phys. **11**, 1 (1960).
[3] R. P. Feynman, *Photon-hadron interactions*, (Benjamin, Reading 1972), 282 p.
[4] A. Donnachie and P. V. Landshoff, Phys. Lett. B **296**, 227 (1992) [hep-ph/9209205].
[5] A. Donnachie and P. V. Landshoff, Phys. Lett. B **348**, 213 (1995) [hep-ph/9411368].
[6] I. P. Ivanov, N. N. Nikolaev and A. A. Savin, Phys. Part. Nucl. **37**, 1 (2006) [hep-ph/0501034].
[7] V. N. Gribov, Sov. Phys. JETP **30**, 709 (1970) [Zh. Eksp. Teor. Fiz. **57**, 1306 (1969)].
[8] J. J. Sakurai and D. Schildknecht, Phys. Lett. B **40**, 121 (1972).
[9] H. Fraas, B. J. Read and D. Schildknecht, Nucl. Phys. B **86**, 346 (1975).
[10] R. J. Glauber, Lectures in Theoretical Physics, vol. 1, pp 315-414, ed. W.E. Brittin, L.G. Dunham, Interscience Publisher Inc. New-York, 1959.
[11] J. Adam *et al.* [ALICE Collaboration], arXiv:1503.09177 [nucl-ex].
[12] C. Adler *et al.* [STAR Collaboration], Phys. Rev. Lett. **89**, 272302 (2002) [nucl-ex/0206004].
[13] B. I. Abelev *et al.* [STAR Collaboration], Phys. Rev. C **77**, 034910 (2008) [arXiv:0712.3320 [nucl-ex]].
[14] G. Agakishiev *et al.* [STAR Collaboration], Phys. Rev. C **85**, 014910 (2012) [arXiv:1107.4630 [nucl-ex]].
[15] L. Frankfurt, M. Strikman and M. Zhalov, Phys. Lett. B **537**, 51 (2002) [hep-ph/0204175].
[16] L. Frankfurt, M. Strikman and M. Zhalov, Phys. Rev. C **67**, 034901 (2003) [hep-ph/0210303].
[17] V. Rebyakova, M. Strikman and M. Zhalov, Phys. Lett. B **710**, 647 (2012) [arXiv:1109.0737 [hep-ph]].
[18] V. N. Gribov, Sov. Phys. JETP **29**, 483 (1969) [Zh. Eksp. Teor. Fiz. **56**, 892 (1969)].
[19] C. Ciofi degli Atti, *et al.*, Phys. Rev. C **84**, 025205 (2011) [arXiv:1105.1080 [nucl-th]].
[20] V. A. Karmanov and L. A. Kondratyuk, Pisma Zh. Eksp. Teor. Fiz. **18**, 451 (1973).
[21] L. G. Dakhno, Sov. J. Nucl. Phys. **37**, 590 (1983) [Yad. Fiz. **37**, 993 (1983)].
[22] U. Dersch *et al.* [SELEX Collaboration], Nucl. Phys. B **579**, 277 (2000) [hep-ex/9910052].
[23] M. L. Good and W. D. Walker, Phys. Rev. **120**, 1857 (1960).
[24] H. I. Miettinen and J. Pumplin, Phys. Rev. D **18**, 1696 (1978).
[25] B. Z. Kopeliovich, L. I. Lapidus and A. B. Zamolodchikov, JETP Lett. **33**, 595 (1981).
[26] B. Blaettel, *et al.*, Phys. Rev. D **47**, 2761 (1993).
[27] L. L. Frankfurt, G. A. Miller and M. Strikman, Ann. Rev. Nucl. Part. Sci. **44**, 501 (1994) [hep-ph/9407274].
[28] D. R. Harrington, Phys. Rev. C **52**, 926 (1995) [nucl-th/9503006].
[29] R. M. Weber, DISS-ETH-16709.
[30] A. J. Baltz, *et al.*, Phys. Rept. **458**, 1 (2008) [arXiv:0706.3356 [nucl-ex]].
[31] J. L. Friar and J. W. Negele, Nucl. Phys. A **212**, 93 (1973).
[32] J. L. Friar and J. W. Negele, In *Adv. Nucl. Phys., Vol.8*, New York 1975, 219-376.
[33] G. D. Alkhazov, S. L. Belostotsky and A. A. Vorobev, Phys. Rept. **42**, 89 (1978).
[34] J. Park, *et al.*, Nucl. Phys. B **36**, 404 (1972).
[35] D. Aston *et al.* Nucl. Phys. B **209**, 56 (1982).
[36] R. M. Egloff, *et al.*, Phys. Rev. Lett. **43**, 657 (1979).
[37] M. Derrick *et al.* [ZEUS Collaboration], Z. Phys. C **69**, 39 (1995) [hep-ex/9507011].
[38] M. Derrick *et al.* [ZEUS Collaboration], Z. Phys. C **73**, 253 (1997) [hep-ex/9609003].
[39] J. Breitweg *et al.* [ZEUS Collaboration], Eur. Phys. J. C **2**, 247 (1998) [hep-ex/9712020].
[40] A. Donnachie and P. V. Landshoff, Phys. Lett. B **478**, 146 (2000) [hep-ph/9912312].
[41] E. M. Levin and L. L. Frankfurt, JETP Lett. **2**, 65 (1965).
[42] P. V. Ramana Murthy, *et al.*, Nucl. Phys. B **92**, 269 (1975).
[43] T. J. Roberts, *et al.*, Nucl. Phys. B **159**, 56 (1979).
[44] A. Schiz, *et al.*, Phys. Rev. D **21**, 3010 (1980).
[45] S. Klein and J. Nystrand, Phys. Rev. C **60**, 014903 (1999) [hep-ph/9902259].
[46] L. Frankfurt, V. Guzey and M. Strikman, J. Phys. G **27**, R23 (2001) [hep-ph/0010248].
[47] T. J. Chapin, *et al.*, Phys. Rev. D **31**, 17 (1985).
[48] E. J. Moniz and G. D. Nixon, Annals Phys. **67**, 58 (1971).
[49] V. P. Goncalves and M. V. T. Machado, Phys. Rev. C **84**, 011902 (2011) [arXiv:1106.3036 [hep-ph]].
[50] G. Sampaio dos Santos and M. V. T. Machado, Phys. Rev. C **91**, no. 2, 025203 (2015) [arXiv:1407.4148 [hep-ph]].
[51] A. M. Breakstone, D. C. Cheng, D. E. Dorfan, A. A. Grillo, C. A. Heusch, V. Palladino, T. Schalk and A. Seiden *et al.*, Phys. Rev. Lett. **47** (1981) 1778.
[52] M. Alvioli and M. Strikman, Phys. Lett. B **722**, 347 (2013) [arXiv:1301.0728 [hep-ph]].
[53] The ATLAS collaboration, ATLAS-CONF-2013-096, ATLAS-COM-CONF-2013-117.